EVALUATION OF ANALYTIC DEFLECTION-LIMITING COMMANDS

Michael Robertson
William Singhose

G.W.Woodruff School of Mechanical Engineering
Georgia Institute of Technology
Atlanta, GA 30332

Abstract: Command signals that can move a flexible system without residual vibration and also limit the transient deflection are very useful, but difficult to create. Historically, these types of commands have been generated via numerical optimization. A method for analytically creating deflection-limiting commands is described and evaluated. Characteristics of the command profile are presented as a function of deflection limit and move distance. Experimental results from a large bridge crane demonstrate key results. The major advantage of this method is that the problem is solvable in closed form, rather than via numerical optimization. *Copyright © 2005 IFAC*

Keywords: Aerospace Control, Flexible System, Vibration Reduction, Transient Response

1. INTRODUCTION

An extensive array of control schemes have been developed to control unwanted vibration in flexible systems (Ben-Asher, *et al*., 1992; Wie, *et al*., 1993; Asada *et al*., 1990; Cannon, and Schmitz, 1984; Papadopoulos, and Garcia, 1997). One approach involves designing a reference command that leads to low levels of vibration (Bhat, and Miu, 1990; Singer and Seering, 1990; Liu, and Wie, 1992). One of the more successful approaches is to generate a reference command that drives the system to cancel out its own vibration. The earliest incarnation of this self-canceling command generation was developed in the 1950's by O.J.M. Smith (Smith, 1958). His posicast control method involved breaking a step of certain magnitude into two smaller magnitude steps, one of which is delayed one-half period of vibration. Unfortunately, his technique was sensitive to modeling errors (Tallman and Smith, 1958). In 1990 Singer and Seering developed reference commands that were robust enough to be effective on a wide range of systems (Singer and Seering, 1990). Their technique is known as input shaping and many useful extensions have been made to their original formulation.

Input shaping is implemented by convolving a sequence of impulses, know as the input shaper, with a desired system command to produce a shaped input that is then used to drive the system. This process is demonstrated in Figure 1. The amplitudes and time locations of the impulses are determined by solving a set of constraint equations that attempt to control the dynamic response of the system. The elimination of the unwanted vibration comes at the expense of the system's rise time. The rise time is delayed by the shaper's duration, Δ. Therefore, it is always desirable to create shapers with the shortest duration possible.
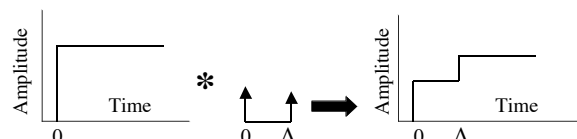

Figure 1: Input Shaping Example.

The constraint on residual vibration amplitude can be expressed as the ratio of residual vibration amplitude with shaping to that without shaping. The percentage vibration can be determined by using the expression for residual vibration of a second-order harmonic oscillator of frequency ω and damping ratio ζ. The vibration from a series of impulses is divided by the

vibration from a single impulse to get the percentage vibration:

$$V(\omega,\zeta) = e^{-\zeta\omega t_n}\sqrt{[C(\omega,\zeta)]^2 + [S(\omega,\zeta)]^2} \text{ , (1)}$$

where,

$$C(\omega,\zeta) = \sum_{i=1}^{n} A_i e^{\zeta\omega t_i}\cos\left(\omega\sqrt{1-\zeta^2}\,t_i\right) \text{ ,} \quad (2)$$

and

$$S(\omega,\zeta) = \sum_{i=1}^{n} A_i e^{\zeta\omega t_i}\sin\left(\omega\sqrt{1-\zeta^2}\,t_i\right) \text{ .} \quad (3)$$

If $V(\omega,\zeta)$ is set equal to zero at the modeling parameters, (ω_m, ζ_m), then a shaper that satisfies the equation is called a Zero Vibration (ZV) shaper. This is the type of solution proposed by Smith in the 1950's.

A ZV shaper will not work well on many systems because it will be sensitive to modeling errors. Therefore, the constraint equations must ensure robustness to modeling errors. Singer and Seering's robust input shaping was achieved by setting the derivative with respect to the frequency of the residual vibration equal to zero. The resulting shaper is called a Zero Vibration and Derivative (ZVD) shaper. The improved robustness can be seen by plotting sensitivity curves – amplitude of vibration *vs*. modeling error, as shown in Figure 2. The normalized frequency is on the abscissa while the percent residual vibration as defined by (1) is on the ordinate. Robustness can be quantified by measuring the insensitivity of the command. The insensitivity, I, is defined to be the nondimensional width of the sensitivity curve that lies below the toleration limit. (For all cases shown here the vibration tolerance is set to 5%.)
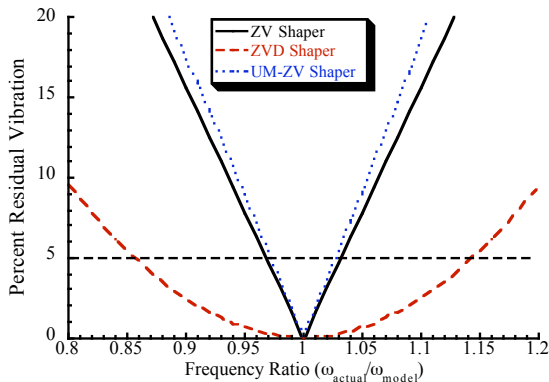

Figure 2: Sensitivity Curves.

Many shapers are derived using the constraint of positive impulse amplitudes to keep the amplitudes from going to positive and negative infinity. An alternative constraint requires that the impulses have unity magnitude. A Unity Magnitude, Zero Vibration (UM-ZV) shaper has a shorter duration than the standard ZV shaper. Figure 3 shows a step command shaped with a UM-ZV shaper.
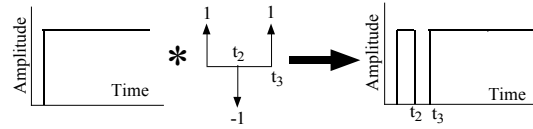

Figure 3: Unity Magnitude, Zero Vibration Command Shaper.

Solving the input shaping constraint equations often requires a nonlinear optimization. However, input shapers can be designed in the digital domain, rather than the continuous domain, to eliminate the need for a nonlinear optimization (Murphy and Watanabe, 1992; Magee and Book, 1993; Tuttle and Seering, 1997; Robertson and Singhose, 2001). This characteristic of digital shaping is extremely useful. Eliminating the need for the nonlinear optimization greatly simplifies the process used to create the commands. However, even a linear optimization may require significant computational effort for some of the more complicated shaper applications.

In an effort to avoid the need for numerical optimization, analytic On-Off shaped commands were developed for rest-to-rest maneuvers (Singhose *et al.*, 1999). As shown in Figure 4, these commands consist of a transition from rest to acceleration (transition 1), a transition from acceleration to deceleration (transition 2) and finally a transition from deceleration to rest (transition 3). These transitions can be created by using standard input shaper design techniques, while the time between the transitions are determined by the constraints on the rigid-body motion.
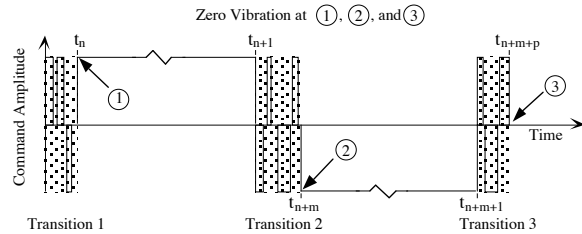

Figure 4: Analytic ON-OFF Commands.

2. DEFLECTION-LIMITING COMMANDS

While these commands successfully eliminated vibration, they could create large deflections during the move. In an effort to reduce internal stresses that result from these deflections, commands have been developed that place a limit on the transient deflection (Singhose, *et al.*, 1997; Robertson, and Singhose, 2001).

One of the great advantages of input shaping is that it requires only simple system models like the one shown in Figure 5. Simple models can be used because input shaping can be made robust to modeling errors. The robustness allows the command profiles developed for simple systems to work effectively on more complex systems.
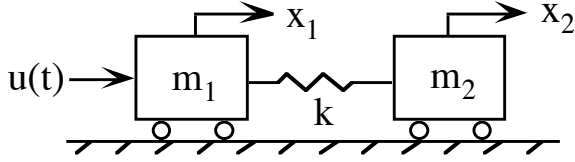
Figure 5: Mass-Spring-Mass Model.

The amplitudes and time locations of the impulses in an input shaper are determined by satisfying a set of constraint equations while minimizing the maneuver duration. Typical constraints are as follows:

1) Residual Vibration Constraints
2) Robustness Constraints
3) Requirement of Time-Optimality
4) Rigid-Body Contraints
5) Constraints on Impulse Amplitude

Solution of the above constraints will lead to commands that eliminate residual vibration and have some level of robustness to modeling errors. However, the deflection of the system during the slew is not specifically limited. If the deflection is large, then the system may be damaged, or the endpoint may deviate considerably from an intended trajectory. In order to control the level of deflection during the move, an expression for the deflection as a function of the input shaper must be obtained. The desired function can be generated using superposition of deflections from individual step inputs. For the system shown in Figure 5, an expression for the deflection is given by:

$$D(t) = D_{(m)-(m-1)}(t)$$
$$= \sum_{i=1}^{m}\left(\frac{D_{max}}{2}\right)a_i\left[\cos(w(t-t_i))-1\right] \quad (4)$$

while,

$$t_m \le t < t_{m+1}, m = 1,\ldots,n \quad (5)$$

where ω is the natural frequency of oscillation

$$\omega = \sqrt{\left(\frac{m_1 + m_2}{m_1 m_2}\right)k} \quad (6)$$

and the coefficient, D_{max}, is given by:

$$D_{max} = \frac{2u_{max}m_2}{k(m_1 + m_2)} \quad (7)$$

It is important to note the restriction presented by the qualifier $t_m \le t < t_{m+1}$ in (5). The deflection which occurs between the first and second impulses of the input, $D_{1-2}(t)$, (the period during the first pulse) is given by (4) when m = 1. The deflection, $D_{2-3}(t)$, between the second and third impulses is given by (4) when m = 2. The deflection, $D_{3-4}(t)$, that occurs during the second pulse is given by (4) with m = 3, etc. Equation 4 amounts to a piecewise-continuous function composed of n finite length segments; each

of the segments has a limited range of applicability. Note that the magnitude of deflection caused by a series of pulses can exceed D_{max} if the deflection components from individual pulses interfere constructively.

3. ANALYTIC DEFLECTION-LIMITING COMMANDS

Even in the absence of vibration, a deflection of magnitude $\Sigma A_i D_{max}/2$, will occur when force is being applied to the system. For the deflection to be limited, the following constraints must be met,

$$\frac{D_{max}}{2}\sum_{i=1}^{m}a_i\left[\cos(w(t-t_i))-1\right] \le Deflim \quad (8)$$

This constraint applies during the times between transition 1 and 2 and between transition 2 and 3 and Deflim is the deflection limit. This can be acccomplished by modifying the impulse amplitude constraint to be

$$\sum a_i = 2\left(\frac{Deflim}{D_{max}}\right) \quad (9)$$

This can be accomplished by modifying a standard UM-ZV shaper to be of the form shown in Figure 6. Combining the impulse amplitudes shown in Figure 6 and (9) we can solve for a_3:

$$a_3 = 2\left(\frac{Deflim}{D_{max}}\right) \quad (10)$$

The impulse amplitudes set by Figure 6 and (10) can be inserted into (2) and (3), set equal to zero and solved for t_2 and t_3 to yield:

$$t_2 = \cos^{-1}[(0.5*(2-2\frac{Deflim}{D_{max}})^2)]/\omega \quad (11)$$

$$t_3 = \cos^{-1}(\frac{-Deflim}{D_{max}})/\omega \quad (12)$$
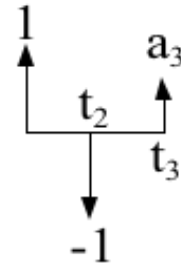

Figure 6: Deflection-Limiting Transition Shaper.

The above equations are used to create command transitions that accelerate the system to its deflection limit without residual vibration. The two-unit

transition (transition 2) is created by using a modified ZV shaper defined by,

$$\begin{bmatrix} a_i \\ t_i \end{bmatrix} = \begin{bmatrix} -a_3 & -a_3 \\ 0 & T/2 \end{bmatrix} \qquad (13)$$

where T is the period of the flexible mode.

With the individual transitions determined by the flexible dynamics, the times between the transitions can be determined by looking at move distance requirements. Considering only the first half of the move for an undamped system (the second half can be found from symmetry), the system must be at the midpoint of the move halfway through the command, or

$$x(t_{mid}) = \frac{x_d}{2} \qquad (14)$$

where x_d is the desired move distance and t_{mid} is described by

$$t_{mid} = t_4 + \frac{T}{4} \qquad (15)$$

By integrating the rigid-body equation of motion with respect to time, an expression t_4 is obtained:

$$t_4 = \frac{(-b + \sqrt{b^2 - 4ac})}{2a} \qquad (16)$$

where

$$a = \alpha * Deflim \qquad (17)$$

$$b = \alpha * (t_2 - 2 * Deflim * t_3 + 2 * Deflim * \frac{1}{4f}) \qquad (18)$$

$$c = -\frac{\alpha}{2} t_2^2 + \alpha * Deflim * t_3^2 + \alpha \left(\frac{1}{4f}\right) t_2 \qquad (19)$$

$$-2 * \alpha * Deflim \left(\frac{1}{4f}\right) * t_3 - \frac{x_d}{2}$$

and α is the force-to-mass ratio. Now the command shaper can by described by

$$\begin{bmatrix} a_i \\ t_i \end{bmatrix} = \begin{bmatrix} 1 & -1 & a_3 & -1 & -1 & a_3 & -1 & 1 \\ t_1 & t_2 & t_3 & t_4 & t_5 & t_6 & t_7 & t_8 \end{bmatrix} \qquad (20)$$

with a_3, t_2, t_3 and t_4 defined by (10), (11), (12) and (16), respectively, and t_5, t_6, t_7 and t_8 determined from symmetry. These equations show that a_3 is proportional to the deflection limit, while the impulse time locations are functions of the deflection limit and the system parameters. Figure 7 shows the command resulting from this formulation.
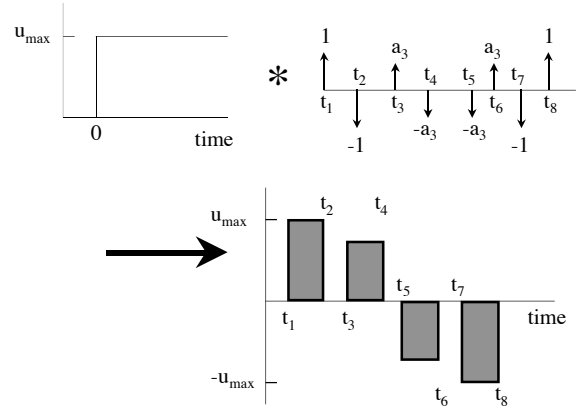

Figure 7: Analytic Deflection-Limiting Command.

4. RESULTS

Simulations were conducted on the benchmark system shown in Figure 5. All the parameters were set to unity, yielding a system with a force-to-mass ratio of 0.5 and a natural frequency of 0.2251 Hz. Three commands were generated to move the system 5 units. The first is a vibration-free analytic on-off command (Singhose et al., 1999). The other commands were designed to have a deflection limit of 0.4, or 80% of the vibration-free deflection obtained using analytic on-off commands and 0.3, or 60% of the vibration-free deflection obtained using analytic on-off commands. Figure 8 shows the input and deflection response for these commands. Note that the first pulse is shortened and the amplitude of the middle pulses are reduced to limit the deflection to the pre-specified limit.
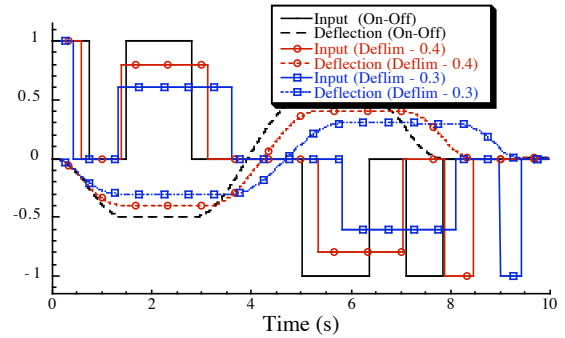

Figure 8: Move distance = 5 units.

The closed-form deflection limiting commands were verified on a 10-ton bridge crane at Georgia Tech. An overhead camera was used to record the position of the payload and the payload's deflection relative to the overhead trolley. Figure 9 shows the position of the payload for four different input commands. The Bang-Bang command has the fastest rise time, but the crane payload oscillates about the desired position after the conclusion of the command. The Fuel-Efficient command was created using the analytic On-Off commands presented earlier, while the deflection-limiting commands were developed to

reduce the transient deflection to 80% and 60% of the vibration-free deflection. Figure 10 shows that the deflection-limiting commands successfully reduce the transient deflection as predicted.
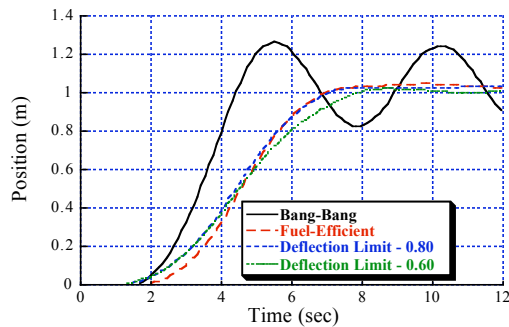

Figure 9: Payload Position.

Figure 10: Payload Deflection.

Figure 11: Robustness as a function of move distance.

Figure 12: Transient Robustness Sensitivity.

In traditional input shaping methods, a shaper's robustness, or insensitivity, is independent of the move distance. However, the insensitivity is dependent on the move distance for analytic on-off and deflection-limiting commands. Figure 11 shows the 5% Insensitivity as a function of move distance for an analytic on-off command and analytic deflection-limiting commands with deflection limits of 0.4 and 0.3. The insensitivity varies greatly with move distance. This occurs because in the presence of modeling errors, there will be some residual vibration at the end of each transition. There will be times when the residual vibrations will interfere destructively, creating an overall command that is more robust than each individual transition. There will also be times when the residual vibrations will interfere constructively, creating an overall command that is less robust than each individual transition. Because the times between the transitions are determined by the rigid-body move distance constraints, the robustness of the command is a function of the move distance.

The transient deflection robustness of analytic commands deflection-limiting commands must be investigated in addition to the residual vibration. Deflection-limiting commands are needed because the transient performance is a critical consideration. Figure 12 shows the effect modeling errors have on the maximum deflection during the move. The percent the maximum deflection exceeded the deflection limit of 0.4 is plotted versus the normalized frequency. For all the move distances shown, overestimating the natural frequency (the model frequency is higher than the actual frequency) always leads to commands that exceed the deflection limit. Underestimation of the natural frequency, however, has negative effects only in some cases.
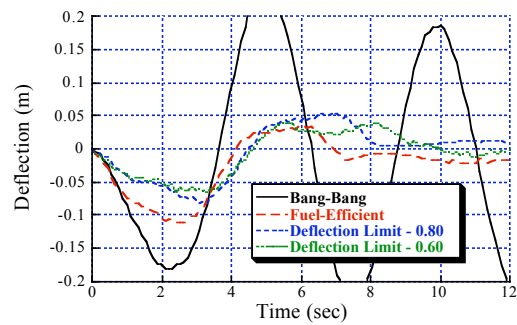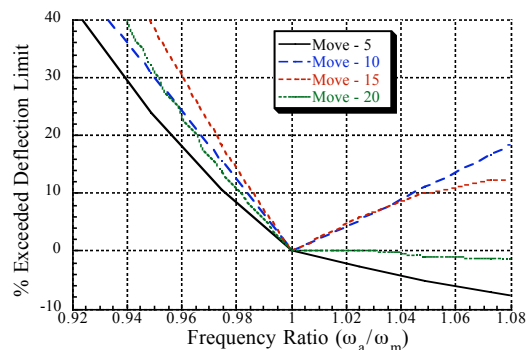
5. CONCLUSIONS

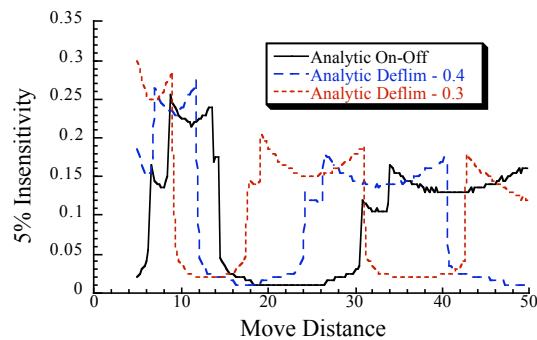A closed-form method for calculating deflection-limiting commands has been developed. The flexible mode is used to determine the zero-vibration transitions, the deflection constraint is used to determine the amplitudes of the transitions, and the move distance constraint is used to determine the times between the transitions. The robustness of these commands is dependent on the move distance. Experimental tests on a large bridge crane verified the effectiveness of the proposed method.

REFERENCES

Asada, H., Z.-D. Ma, and H. Tokumaru (1990). Inverse Dynamics of Flexible Robot Arms: Modeling and Computation for Trajectory Control. *J. of Dynamic Systems, Measurement, and Control*, **vol. 112**, pp. 177-185.

Ben-Asher, J., J. A. Burns, and E. M. Cliff (1992). Time-Optimal Slewing of Flexible Spacecraft. *J. of Guidance, Control, and Dynamics*, **vol. 15**, pp. 360-367.

Bhat, S. P., and D. K. Miu (1990) Precise Point-to-Point Positioning Control of Flexible Structures. *J. of Dynamic Sys., Meas., and Control*, **vol. 112**, pp. 667-674.

Cannon, R. H. and E. Schmitz (1984). Initial Experiments on the End-Point Control of a Flexible One Link Robot. *Int. J. of Robotics Research*, **Vol. 3**

Liu, Q. and B. Wie (1992). Robust Time-Optimal Control of Uncertain Flexible Spacecraft. *J. of Guidance, Control, and Dynamics*, **vol. 15**, pp. 597-604.

Magee, D and W. Book (1993). Implementing Modified Command Filtering to Eliminate Multiple Modes of Vibration. American Control Conference, San Francisco, CA.

Murphy , B. R. and I. Watanabe (1992). Digital Shaping Filters for Reducing Machine Vibration. *IEEE Transactions on Robotics and Automation*, **vol. 8**, pp. 285-289.

Papdopoulos, M. and E. Garcia (1997). Closed-Loop Pole Design for Vibration Suppression. *Journal of Guidance, Control and Dynamics*, **vol. 20**, pp. 333-337.

Robertson, M and W. Singhose (1999). Initial Guess Schemes for Generating Deflection-Limiting Commands. AAS/AIAA Astrodynamics Specialist Conference, Girdwood, AK.

Robertson, M and W. Singhose (2001). Generating Deflection-Limiting Commands in the Digital Domain. AAS/AIAA Astrodynamics Specialist Conference, Quebec City, Quebec, Canada.

Robertson, M and W. Singhose (2001). Multi-level Optimization Techniques for Designing Digital Shapers. American Control Conference, Pittsburgh, PA.

Singer, N. C., and W. P. Seering (1990). Preshaping Command Inputs to Reduce System Vibration. *J. of Dynamic Sys., Measurement, and Control*, **vol. 112**, pp. 76-82.

Singh, T. and S. R. Vadali (1994). Robust Time-Optimal Control: A Frequency Domain Approach. *J. of Guidance, Control and Dynamics*, **vol. 17**, pp. 346-353.

Singhose, W., A. Banerjee, and W. Seering (1997). Slewing Flexible Spacecraft with Deflection-Limiting Input Shaping. *AIAA J. of Guidance, Control, and Dynamics*, **vol. 20**, pp. 291-298.

Singhose, W., B. Mills, and W. Seering, (1999). Closed-Form Methods for Generating On-Off Commands for Undamped Flexible Structures. *AIAA J. of Guidance, Control, and Dynamics*, **vol. 22**.

Smith, O. J. M. (1958). *Feedback Control Systems*. McGraw-Hill Book Co., Inc., New York

Tallman, G. H. and O. J. M. Smith (1958). Analog Study of Dead-Beat Posicast Control. *IRE Transactions on Automatic Control*, pp. 14-21.

Tuttle T. D. and W. P. Seering (1994) A Zero-placement Technique for Designing Shaped Inputs to Suppress Multiple-mode Vibration. *American Control Conference*, Baltimore, MD.

Wie B., R. Sinha, and Q. Liu (1993). Robust Time-Optimal Control of Uncertain Structural Dynamic Systems. *J. of Guidance, Control, and Dynamics*, **vol. 15**, pp. 980-983.